# Self-localization Method Using Time-of-arrival and Direction-of-arrival of Sound Waves Measured Based on the Doppler Effect

Atsushi Tsuchiya†‡, Naoto Wakatsuki*, Tadashi Ebihara, Keiichi Zempo and Koichi Mizutani (Univ. Tsukuba)

## 1. Introduction

Mobile robots have been introduced at construction sites and factories. For a mobile robot to estimate its position, it is necessary to measure objects using ranging sensors. Light detection and ranging (LiDAR) and ultrasonic sensors have been introduced as typical ranging sensors. LiDAR can measure a wide angular range with high angular resolution. However, false positives are more likely to occur in environments with optical scatterers. In such cases, an ultrasonic sensor is expected to have the ability to correct the measurement. Generally, an ultrasonic sensor capable of ranging over a wide angular range is realized by applying array signal processing to multiple ultrasonic transducers. However, this system requires much cost due to the large size of the device and the need for multiple channels of analog input.

Therefore, we have been studying sensing devices that can measure distances in all directions using only a single acoustic channel[1]. When only one acoustic channel is used, it is usually impossible to know the direction of arrival of the reflected wave. On the other hand, if the sensor is moving, a Doppler shift occurs in the received signal. This sensor reveals the direction of arrival of the reflected wave by measuring this Doppler shift[2].

In this paper, we propose a method for estimating the mobile robot's self-position using the ttime-of-arrival and direction-of-arrival of reflected waves measured based on the Doppler effect. The sensing and self-positioning estimation methods proposed in this paper are implemented in a simulation and evaluated numerically in a two-dimensional space.

## 2. Proposed methods

### 2.1 Measurement of reflected waves

The time-of-arrival and direction-of-arrival of the reflected wave were measured using pulse compression, which considers the Doppler effect[2]. This method uses a single loudspeaker and a single microphone. Pulse compression considering the Doppler shift, computes the cyclic cross-correlation between the received signal with its time scale stretched or shrunk and the transmitted signal. If the moving speed of the mobile robot is known and the wall surface is not moving, the magnitude of the Doppler shift can be related to the direction of arrival of the reflected wave. Based on this information, the distance and direction from the current position of the mobile robot to the wall is visualized as a two-dimensional image.

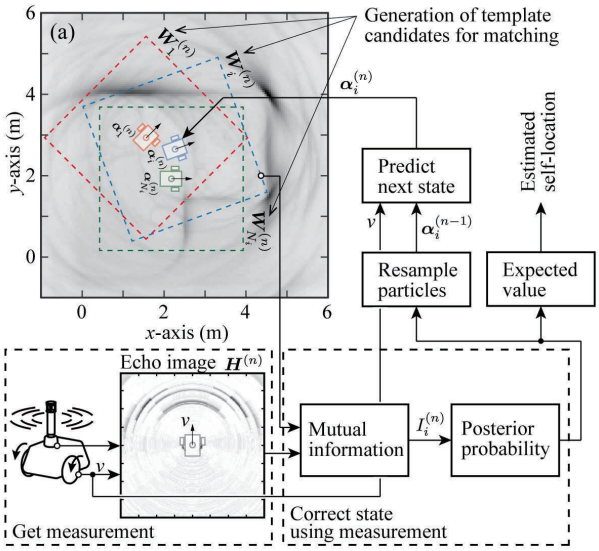


Fig. 1 Schematic diagram of proposed method. (a) is a map generated by mapping methods.

### 2.2 Mapping method

In this method, a map is created in advance and used for self-position estimation. In the mapping phase, the mobile robot is operated along a predetermined path, and the results of reflected wave measurements are recorded. During the mapping phase, it is assumed that the position coordinates of the mobile robot at the time of the reflected wave measurement can be obtained from different sensors, such as cameras. The reflected wave measurement results described in **2.1** are converted to global coordinates using each coordinate and the orientation of the mobile robot. Each pixel value of the completed map is the sum of the pixel values of the reflected wave measurement images corresponding to the coordinates of each pixel of the completed map. **Fig. 1**(a) shows an example of the map image created.

E-mail: †tsuchiya@aclab.esys.tsukuba.ac.jp, *wakatuki@iit.tsukuba.ac.jp

### 2.3 Self-localization method

An overview of the self-position estimation method is shown in Fig. 1. We introduced a particle filter for the self-position estimation algorithm. The particle filter is a method to obtain a probabilistic estimate of self-position by sequentially updating multiple candidate self-position. When the candidate self-position estimated one step ago is $\boldsymbol{\alpha}_i^{(n-1)}$, the current candidate self-position $\boldsymbol{\alpha}_i^{(n)} = (x_i^{(n)} \quad y_i^{(n)} \quad \phi_i^{(n)})^T$ is predicted using the measured wheel angular velocity of the mobile robot. Where $i$ is the candidate subscript, $n$ is the time step, $x$, $y$ are the global coordinates of the self-position, and $\phi$ is the mobile robot's travel direction. A candidate image $W_{i,j}^{(n)}$ for template matching is generated using the predicted candidate self-position and the map created in the mapping phase, where $W_{i,j}^{(n)}$ is the pixel value of the #$j$th pixel in the candidate image. The similarity between the measured image of the reflected wave and the candidate template images is calculated. We introduced the mutual information for calculating the similarity. The mutual information content is expressed by

$$I_i^{(n)} = \sum_{k_1=1}^{K} \sum_{k_2=1}^{K} P_{WH}(k_1, k_2) \log \left( \frac{P_{WH}(k_1, k_2)}{P_W(k_1) P_H(k_2)} \right), \qquad (1)$$

where, $P_{WH}(k_1, k_2) = P(W_{i,j}^{(n)} = k_1, H_j^{(n)} = k_2)$ , $P_W(k_1) = P(W_{i,j}^{(n)} = k_1)$ and $P_H(k_2) = P(H_j^{(n)} = k_2)$. $P()$ represents the probability. $H_j^{(n)}$ is the pixel value of the #$j$th pixel in the measured reflected wave image. $K$ is the maximum pixel value. The posterior probability of a candidate self-position predicted using similarity is calculated. The result of calculating the expected value using the posterior probability of the predicted candidate point is the estimated self-position. The posterior probabilities are used to resample the candidate point set from the predicted candidate point set for the next step. This procedure is repeated to obtain an estimate of self-position.

### 3. Simulation setup and results

We introduced a two-dimensional finite-difference time-domain (FDTD) method as our simulation method[3]: the grid width of the FDTD method is $5$ mm, the time step width is $8.333$ μs, the number of analysis cells is $1000 \times 1000$ cells, the sound velocity is $340$ m/s, and the density is $1.293$ kg/m$^3$. Four rigid walls were set up, as shown in **Fig. 2**. During the reflected wave measurement, the transmitted waveform is a binary phase-modulated signal with maximal-length-sequence (M-sequence) codes. The carrier frequency is $10$ kHz, the chip rate is $10$ kHz, and the code length is 1023. Fig. 2(a) shows the moving path of the mobile robot during mapping. The map generated by this movement path is shown in Fig. 1(a).

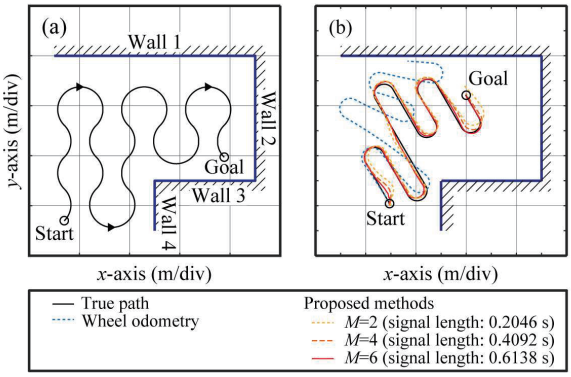


Fig. 2 (a) Moving path of the mobile robot during mapping, (b) estimation results.

Fig. 2(b) shows the results of the self-position estimation. We set an offset error of $0.01$ rad/s in the measured rotational angular velocity of the mobile robot to verify that it is possible to compensate for measurement errors that occur in the movement speed. Therefore, the wheel odometry measurement results deviate significantly from the actual path. The proposed method was compared with three different signal lengths for cyclic cross-correlation during reflected wave measurement: $M$=1 represents the time when the M-sequence code has one period, and the signal length is $0.1023$ s. The estimation results for $M$=2 deviate significantly from the actual path. The estimated results of $M$=4 and $M$=6 are close to the actual paths. This result is attributed to the improved detection performance of the Doppler shift. The enhanced detection performance of the Doppler shift improved the angular resolution of the reflected wave measurement, resulting in enhanced position estimation accuracy.

### 4. Conclusion

we proposed a method for estimating the mobile robot's self-position using the time-of-arrival and direction-of-arrival of reflected waves measured based on the Doppler effect. We showed by simulation that the self-position estimation is possible when the signal length is long enough.


### Acknowledgment

This work was supported by JSPS KAKENHI Grant Number 22KJ9431.


### References


1) A. Tsuchiya, N. Wakatsuki, T. Ebihara, K. Zempo and K. Mizutani: Jpn. J. Appl. Phys. **61** (2022) SG1037.
2) A. Tsuchiya, N. Wakatsuki, T. Ebihara, K. Zempo and K. Mizutani: Proc. Int. Cong. on Sound and Vibration, 2023, 268
3) T. Tsuchiya and M. Kanamori: Jpn. J. Appl. Phys. 60 (2021) SDDB02.